Lab Invest. Author manuscript; available in PMC 2015 January 01.

Published in final edited form as:

Lab Invest. 2014 July ; 94(7): 716–725. doi:10.1038/labinvest.2014.62.

Granzyme B Releases Vascular Endothelial Growth Factor from Extracellular Matrix and Induces Vascular Permeability

Alon Hendel[1,2], **Ivy Hsu**[1,2], and **David J. Granville**[1,2,*]

[1]Centre for Heart Lung Innovation, St. Paul's Hospital, Vancouver, BC, Canada

[2]Department of Pathology and Laboratory Medicine, University of British Columbia, Vancouver, BC, Canada

Abstract

The formation of unstable, leaky neovessels underlies the pathogenesis of many chronic inflammatory diseases. Granzyme B (GZMB) is an immune-derived serine protease that accumulates in the extracellular matrix (ECM) during chronic inflammation and is capable of cleaving fibronectin (FN). Vascular endothelial growth factor (VEGF) is a potent vascular permeabilizing agent that is sequestered in the ECM through its interaction with FN. As GZMB levels are elevated in chronic inflammatory diseases that are associated with increased vascular permeability, the role of GZMB in the regulation of VEGF bioavailability and vascular permeability were assessed.

Methods and Results—GZMB was added to either VEGF-bound to FN or VEGF-bound to endothelial cell (EC)-derived ECM. Supernatants containing released VEGF were assessed to determine VEGF activity by treating EC and evaluating VEGF receptor-2 (VEGFR2) phosphorylation. GZMB released VEGF from both FN and from EC-derived matrix, while GZMB inhibition prevented FN cleavage and VEGF release. GZMB-mediated VEGF release resulted in significant phosphorylation of VEGFR2. The role of GZMB-mediated VEGF release in altering vascular permeability was also assessed *in vivo* using a Miles/Evan's Blue permeability assay. GZMB induced a significant VEGF-dependent increase in vascular permeability *in vivo* that was reduced in the presence of an anti-VEGF neutralizing antibody. Inflammatory-mediated vascular leakage was also assessed in GZMB-KO mice using a delayed-type hypersensitivity model. GZMB-KO mice exhibited reduced microvascular leakage compared to C57\B6 controls.

Conclusions—GZMB increases vascular permeability in part through the proteolytic release of ECM-sequestered VEGF leading to VEGFR2 activation and increased vascular permeability *in vivo*. These findings present a novel role for GZMB as a modulator of vascular response during chronic inflammation.

*Corresponding author: David J. Granville, Centre for Heart Lung Innovation, St. Paul's Hospital, University of British Columbia. Rm 166, Burrard Building, 1081 Burrard Street, Vancouver, BC. V6Z 1Y6, Canada. Phone: (604) 806-9267, Fax: (604) 806-9274, David.Granville@hli.ubc.ca.

Disclosures: Dr. Granville is a member of the scientific advisory board and serves as the Chief Scientific Officer to viDA Therapeutics.

Keywords

Fibronectin; Granzyme B; Inflammation; VEGF; Vascular permeability

Increased vascular permeability is one of the earliest manifestations of inflammation resulting in extravasation of protein-rich plasma into the affected tissue. Acute vascular permeability allows the deposition of circulating plasma matrix proteins including fibrin and fibronectin (FN) which facilitate cell migration into the inflamed area [1]. This process also provides an access point for immune cells and immunoglobulins to enter the tissue and help fight foreign antigens [2]. In contrast, chronic vascular hyperpermeability is suggested to sustain the inflammatory response and delay resolution, further exacerbating chronic inflammation [2, 3]. This type of vascular hyperpermeability underlies the pathogenesis of a large number of chronic disorders including rheumatoid arthritis (RA), psoriasis, ocular disease, cancer and chronic wounds [2, 3].

Vascular endothelial growth factor (VEGF) is a potent vascular permeabilizing agent that is highly expressed during chronic inflammation and contributes to pathological angiogenesis [4]. VEGF induces vascular leakage by activating VEGF receptor 2 (VEGFR2)-mediated signaling events in endothelial cells (EC) leading to plasma extravasation [5]. Cellular sources for VEGF during inflammation may include macrophages and mast cells; however it can also be expressed by EC and acts in a paracrine and autocrine fashion [6].

The extracellular matrix (ECM) has a major role in regulating VEGF bioavailability. VEGF contains a cluster of basic residues that facilitate its interaction with anionic ECM proteins [7]. VEGF interaction with the ECM greatly determines its bioavailability as the majority of VEGF is retained in the ECM after cell secretion [7]. Other proteases may alter VEGF interaction with the ECM including plasmin [7] and MMPs [8, 9], giving rise to increased microvessel leakage and formation of aberrant neovasculature that is characteristic of pathological angiogenesis [8]. Thus, ECM-sequestered VEGF can be liberated by proteases and this process has significant implications on vascular integrity. Importantly, VEGF binds to the growth factor binding domain in FN [10–12]. Binding of VEGF to FN enhances EC migration, proliferation, and promotes angiogenesis [10, 11, 13]. However, the consequences of VEGF release from FN by a specific protease and its impact on vascular integrity has yet to be explored.

Granzyme B is a serine protease that is primarily expressed by immune cells including lymphocytes, macrophages, neutrophils, and mast cells [14]. Although traditionally viewed as a pro-apoptotic intracellular protease used by cytotoxic lymphocytes to induce target cell apoptosis, we and others have demonstrated the important role of extracellular GZMB activity in a number of chronic inflammatory diseases (reviewed in [15, 16]). GZMB accumulates in the ECM of inflamed tissues and is present in several bodily fluids in chronic diseases such atherosclerosis, chronic obstructive pulmonary disease (COPD) and RA [17, 18]. ECM proteolysis by GZMB leads to impaired tissue integrity in diseases. In a murine mouse model of abdominal aortic aneurysm (AAA), GZMB cleavage of fibrillin-1 and decorin results in increased AAA rupture [19, 20]. In addition, degradation of decorin and FN by GZMB leads to increased skin thinning and delayed wound healing in apolipoprotein

E-knockout (KO) mice [21, 22]. Moreover, extracellular GZMB is suggested to potentiate pro-inflammatory cytokine activities as it converts the pro form of IL-18 to its active form leading to increased IFN-γ release from human keratinocytes [23]. GZMB cleavage of IL-1α results in enhanced pro-inflammatory activity of this cytokine both *in vitro* and *in vivo* [24]. Interestingly, GZMB cleavage of decorin, biglycan and betaglycan leads to release of TGF-β1 from the matrix, suggesting that GZMB may indirectly affect normal cell function by altering growth factor bioavailability [25].

We have previously demonstrated that GZMB cleavage of FN dysregulates angiogenesis by impairing EC adhesion, migration and capillary formation [26]. The present study explores the effects of GZMB-mediated FN proteolysis on VEGF bioavailability and activity. We hypothesized that GZMB-mediated FN cleavage releases VEGF from the ECM and promotes vascular leakage.

Materials and Methods

VEGF release assay

48 well plates were coated with human purified plasma FN (20 μg/ml) (Sigma St. Louis, MO) in DPBS for 1 h at 37°C. Wells were then blocked with 1% BSA in DPBS for 30 min at 37°C. VEGF 165 (50ng/ml) (R&D systems, Minneapolis, MN) was added to the FN coated wells and incubated for 2 h at 37°C followed by extensive washing to remove unbound VEGF. Human purified GZMB (50 nM) (Axxora, San Diego, CA) in Tris buffer (50mM Tris, pH=7.4) with either vehicle control (1:100 DMSO) or GZMB inhibitor (Compound 20 (50μM), UBC Centre for Drug Research and Development, Vancouver, BC) [27] were added to the well for additional 2 h at 37°C. Supernatants were analysed by VEGF ELISA (R&D systems, Minneapolis, MN) according to the manufacturer instruction. For VEGF release from human umbilical vein endothelial cells (HUVEC) matrix, HUVEC were cultured in a 6 well plate and grown to confluence in complete growth media (EGM2+2%FBS) (Clonetics/Lonza, Walkersville, MD). Cells were maintained in serum-reduced (0.2% FBS) media for 9 d and media was changed every 2 d. To remove the cells while leaving the ECM intact, cells were washed 3 times with DPBS and 200 μl/ well of 0.25 M ammonium hydroxide was added and incubated for 20 min at RT. Wells were washed 3 times with dH_2O and cell removal was confirmed by microscopical examination. Remaining ECM was then blocked with 1% BSA for 30 min at 37°C, followed by addition of VEGF (50 ng/ml) in 1% BSA for 2 h at 37°C. Unbound VEGF was removed by washing the wells with DPBS and GZMB (50 nM) in Tris buffer with either vehicle control or Compound 20 (UBC Centre or Drug Research and Development, Vancouver, BC) were added to the well for additional 2 h at 37°C. Supernatants were analysed by VEGF ELISA.

FN and VEGF cleavage assay

48 well plates were coated with FN as described above. GZMB (50nM), plasmin (50nM), GZMB (50nM)+compound 20 (50μM), plasmin (50nM)+aprotinin (125nM), GZMB (50nM) +aprotinin (Sigma), were added to the wells in Tris buffer for 2h at 37°C (plasmin was kindly provided by Dr. Ed Pryzdial, University of British Columbia). Enzyme preparations from the above experiment were used for VEGF cleavage assay. GZMB (50nM) or plasmin

(50nM) were incubated with 100ng VEGF in Tris buffer for 2h at 37°C. Supernatants from the FN cleavage assay and the VEGF cleavage assay samples were analysed by western blotting. In brief, samples were resolved by either 10% (for FN supernatants) or 20% (for VEGF samples) SDS-PAGE and gels were transferred to PVDF membranes. Membranes were blocked with 2.5% milk and immunoblotted using anti-human FN Ab (R&D systems, Minneapolis, MN) at 1:1000 dilution in blocking solution or biotinylated anti-human VEGF (R&D systems, Minneapolis, MN) at 1:100 dilution over night at 4°C. FN signal was detected by incubating membrane with IRDye 800 anti-mouse Ab (LI-COR Biosciences, Lincoln, NE) for 1hr at RT and fluorescent signal was imaged using the Li-COR Odyssey Infrared Imaging System (Li-COR Biosciences, Lincoln, NE). VEGF signal was detected by first incubating membrane with ABC reagent (Vector Laboratories Inc., Burlingame CA) for 30min at RT and adding ECL Plus© substrate (GE Healthcare, Buckinghamshire UK). Chemiluminescence signal was captures using Chemigenius Bioimaging System (Syngene, Frederick MD). Mouse FN cleavage assay was performed in the same way as described for human FN, using 48 culture wells coated with mouse FN (20 μg/ml; Sigma St. Louis, MO) treated with either recombinant mouse granzyme B (mGZMB; Sigma St. Louis, MO) or human GZMB.

VEGFR2 phosphorylation by GZMB-mediated VEGF release from FN

HUVEC were grown to confluence in 6 well plate in complete growth media (EGM2+2%FBS). Media was changed to EGM2 no VEGF +1%FBS media for 2 days prior to treating cells with VEGF release supernatants. VEGF release from FN coated wells was performed as described above, however this time treatments were prepared in M199 media (HyClone, Logan, UT) to allow the use of the supernatants as a treatment media for HUVEC culture. VEGF release supernatants were added to HUVEC culture for 7 min followed by rapid cell lysis with lysis buffer (CellLytic M, Sigma St. Louis, MO) that included phosphatase inhibitor cocktail (1:100) and proteinase inhibitor cocktail (1:100) (Sigma St. Louis, MO). Total protein concentration was quantified using BioRad Bradford protein assay (BioRad Laboratories), and 50μg of total protein cell lysates were resolved by 10% SDS PAGE and immunoblotted using pVEGFR2y1214 Ab, pVEGFR2y1175 Ab, total VEGFR2 Ab (Cell Signaling Technology, Danvers, MA) (1:700 dilution in 2.5% milk). β-tubulin immunoblotting was used as a loading control. Densitometry was used to quantify pVEGFR2 and values were divided by the expression levels of total VEGFR2 and normalized to β-tubulin loading control (n=3 with three replicates per treatment).

In vivo permeability assay

Animal procedures described were performed in accordance with the appropriate University of British Columbia (UBC) guidelines for animal experimentation and approved by the UBC Animal Care Committee. 8–10 weeks old CD1 female mice were injected with 200μl Evan's Blue dye (0.5% in injectable saline)(Sigma St. Louis, MO) via the tail vein. The following treatments were prepared in injectable saline to a final volume of 10μl (n=5 for each treatment group): mGZMB (100ng), mGZMB (100ng) + neutralizing anti mouse VEGF antibody (1.5μg; R&D systems, Minneapolis, MN), mGZMB (100ng) + goat IgG control (1.5μg; R&D systems, Minneapolis, MN). Treatments were injected intradermally to the ear. After 30 min mice were euthanized and perfused with saline to clear the circulation from

any remaining dye. Ear tissues were excised using a 7 mm punch biopsy and dried in 60°C incubator overnight. Tissues were weighed and dye was extracted by incubating tissues with 300μl formamide (Sigma St. Louis, MO) in 60°C incubator for 24 h. Absorbance of the extracted dye was measured at 610 nm and values were normalized to tissue weight.

VEGF, FN immunohistochemistry and Immunofluorescence

Formalin-fixed, paraffin-embedded sections of untreated mouse ear tissue were sectioned at 5 μm thickness. Sections were deparaffinised and rehydrated in xylene and decreasing concentrations of ethanol. Antigen retrieval was performed by boiling slides in citrate buffer (pH= 6) (Invitrogen, Carlsbad, CA) for 15 min followed by a 30 min cooling at room temperature. Endogenous peroxides were quenched by incubating sections in 3% H_2O_2 for 15 min. Sections were blocked with 10% rabbit serum for 30 min and incubated over night at 4°C with 10μg/ml goat anti-mouse VEGF Ab (R&D systems, Minneapolis, MN). Sections were incubated with 1:350 dilution of biotinylated rabbit anti-goat Ab for 30 min followed by signal amplification using Vectastain® ABC system (Vector Laboratories Inc., Burlingame, CA), according to manufacturer's instructions. Staining was visualized using DAB (Vector Laboratories Inc., Burlingame, CA). Images were captured using Nikon Eclipse E600 microscope (Nikon). Mouse kidney sections were used as positive control for VEGF staining. Negative control samples undergo the same treatment without primary Ab incubation. For double immunofluorescence staining for VEGF and FN, untreated mouse ear tissue sections were blocked with 10% donkey serum for 1 h and co-incubated over night at 4°C with goat anti-mouse VEGF Ab (R&D systems, Minneapolis, MN) and rabbit anti-FN Ab (Abcam, Cambridge, MA) diluted at 1:20 and 1:500, respectively. Sections were then incubated for 1 h with donkey anti-goat Alexa 594 Ab for VEGF detection, and with donkey anti-rabbit Alexa 488 Ab for FN detection (1:350 dilution, Invitrogen, Carlsbad, CA). Fluorescent images were captured using Leica Upright Fluorescence Microscope with Fast Confocal Scanner and CCD camera (Leica Microsystems, Wetzlar, Germany).

In vivo oxazolone-induced delayed type hypersensitivity (DTH) reaction model

Animal procedures described were performed in accordance with the appropriate University of British Columbia (UBC) guidelines for animal experimentation and approved by the UBC Animal Care Committee. On day 1, 8–11 weeks old C57/BL6 wild type (WT) and GZMB-KO mice were sensitized by applying 2.5% oxazolone (Sigma-Aldrich, St. Louis, MO) dissolved in 4:1 acetone:olive oil topically on shaved abdomen (50 μL) and each paw (25 μL). On day 7, mice were challenged by applying 1% oxazolone dissolved in 4:1 acetone:olive oil topically to each ear (15μL). Vascular permeability was examined after 24h (WT n=8, GZMB-KO n=11) and 72h (WT, n=11; GZMB-KO, n=7) post-challenging by injecting the mice with 400μL Evan's Blue dye (1% in injectable saline) via the inferior vena cava. After 15 min, mice were euthanized and ear tissue collections and analysis were performed as described for the *in vivo* permeability assay.

Statistics

One way analysis of variance (ANOVA) with Bonferroni's multiple comparison post test was performed to determine statistical differences between multiple groups. A paired t test

was performed to determine statistical difference between two matching groups. A value of $P<0.05$ was considered significant.

Results

GZMB releases VEGF from human plasma FN

To examine the ability of GZMB to release VEGF from FN, culture plates were coated with human plasma FN followed by addition of VEGF. VEGF was effectively bound to FN as only a small amount of VEGF spontaneously dissociated to the supernatant in the control group (37.72 pg/ml $\pm$ 23.95) (Figure 1). However, GZMB treatment elicited significant release of VEGF to the supernatant (350 pg/ml $\pm$ 61.35; $P<0.001$). The release of VEGF was dependent on GZMB activity as co-treatment with GZMB inhibitor (Compound 20, UBC Centre for Drug Research and Development, Vancouver, BC) significantly reduced VEGF release (147 pg/ml $\pm$ 8.3; $P<0.05$). Thus, GZMB promotes the release of VEGF from human plasma FN.

GZMB releases VEGF from HUVEC matrix

Since EC-derived ECM is more complex and may contain other pericellular matrix proteins that can bind VEGF [28], it was essential to explore whether GZMB could mediate VEGF release from endogenous matrix. VEGF was added to HUVEC-derived matrix and unbound VEGF was removed by washing. Similar to experiments done on plasma FN, GZMB treatment significantly increased VEGF release from HUVEC matrix compared to control (control 135 pg/ml $\pm$ 33.66; GZMB 562 pg/ml $\pm$ 39.86; $P<0.01$) (Figure 2). Inhibition of GZMB effectively reduced GZMB-mediated VEGF release (275 pg/ml $\pm$ 63.8; $P<0.05$). Thus, GZMB promotes VEGF release from both plasma FN and from endogenously produced matrix.

VEGF is not a proteolytic substrate of GZMB

Several proteases have been demonstrated to release VEGF from the ECM by cleaving VEGF intramolecularly, generating a smaller VEGF fragment with altered biological activity [7, 8, 29, 30]. As such, the status of GZMB-released VEGF from the matrix was assessed. Plasmin was used as a positive control as it is known to cleave VEGF [7]. To first confirm the activity and specificity of plasmin and GZMB, FN release assay was performed by adding either GZMB or plasmin to FN coated culture plates and the supernatants were examined for the release of FN fragments by western blot. Untreated control wells gave rise to a single, faded band corresponding to the full length FN protein that was spontaneously dissociated from the plate during the incubation period. In contrast, GZMB treatment effectively cleaved FN, yielding a number of cleavage fragments that differ in size from those generated by plasmin (Figure 3A). FN cleavage was dependent on the enzymatic activity of both proteases as addition of aprotinin and compound 20 completely prevented FN degradation by plasmin and GZMB, respectively. Interestingly, although aprotinin is a broad range serine protease inhibitor, it did not inhibit GZMB activity. The same enzyme preparations used for the FN release assay were used to examine VEGF proteolysis. As expected, plasmin incubation with VEGF resulted in the generation of a smaller VEGF fragment (Figure 3B, arrow). Conversely, VEGF was not cleaved by GZMB, as no VEGF

fragments were observed upon GZMB treatment (Figure 3B). Thus, the release of VEGF from the ECM by GZMB is not due to an intramolecular cleavage of the VEGF molecule.

GZMB-mediated VEGF release from FN activates VEGFR2

VEGFR2 dimerizes and undergoes rapid transphosphorylation in a number of tyrosine residues upon ligation with VEGF [5]. We were determined to examine whether VEGF that is released from FN by GZMB retains its biological activity. HUVEC were treated with VEGF release supernatants, produced by the addition of GZMB to VEGF-bound FN as in Figure 1, and VEGFR2 activation was examined by immunoblotting for the phosphorylation of Y1214 and Y1175. Even small amounts of VEGF that spontaneously dissociate from FN activate VEGFR2 as control supernatants show distinct signal for both Y1214 and Y1175 phosphorylation, while HUVEC treated with media containing no VEGF (-ve control) show no phosphorylation signal (Figure 4A). However, VEGF release supernatants that were generated due to GZMB activity caused a significant increase in VEGFR2 phosphorylation of both Y1214 and Y1175 (Figure 4A, B). VEGF released from FN treated with GZMB + inhibitor leads to attenuated VEGFR2 activation. Thus, VEGF that is released from FN by GZMB is active and it can effectively lead to VEGFR2 phosphorylation in HUVEC.

GZMB-mediates VEGF dependent vascular permeability in vivo

To test the impact of GZMB-mediated VEGF release on vascular leakage we used the Miles assay [31] by injecting mouse GZMB (mGZMB) to the ear and measured Evan's blue extravasation as described in the Material and Methods. To minimize the background of Evan's blue dye that is present in the circulation and did not extravasate we perfused the animal with large volume of saline (10ml) prior to analyzing the tissue. Vascular leakage at the tip of the ear was due to holding the ear with forceps to stabilize the ear during injections. Only the injection area at the base of the ear was excised with 7 mm punch biopsy for subsequent dye extraction. Absorbance of the extracted dye was normalized to tissue weight. mGZMB injection resulted in increased vascular leakage compared to saline injections (n=5) (Figure 5A). To further establish whether the increase in vascular leakage is dependent on VEGF activity we co-injected mGZMB with anti-mouse neutralizing VEGF Ab. Vascular leakage was significantly reduced when mGZMB was injected with VEGF neutralizing Ab compared to mGZMB + IgG control injections (n=5) (Figure 5B).

To confirm the source of VEGF in the *in vivo* experiments, untreated mouse ear sections were assessed imunohistochemically for VEGF expression. As a positive control, we used mouse kidney sections as VEGF is reported to be expressed at higher levels by podocytes within the glomerulus and to a lesser extent by the cells of the convoluted tubules [32]; an observation that we confirmed in our experiments (Figure 6Aiii). Within the mouse ear, VEGF is expressed in the epidermis and in the deep dermis above the cartilage tissue (Figure 6i). This observation is in line with other studies indicating the importance of basal VEGF expression in the epidermis and dermis to maintain normal permeability barrier homeostasis [33], while increased VEGF levels promote tissue edema and the development of psoriatic skin phenotype in the mouse ear [34]. Immunohistochemical staining for VEGF in the ear revealed intracellular expression within the cells of the epidermis and dermis (Figure 6Bi). Additionally, double immunofluorescence for VEGF and FN indicates that VEGF co-

localizes with FN in the deep dermis (Figure 6Biii). Thus, VEGF was found to co-localize to FN in the mouse ear and serves as a source for the VEGF-dependent vascular leakage observed in the above Miles assay.

As our previous experiments included only human sources for both GZMB and FN, we wanted to confirm whether mGZMB can cleave mouse FN (mFN). FN release assay was preformed as in Figure 3 using mFN treated with either mGZMB or human GZMB (hGZMB). mGZMB effectively cleaves mFN as a number of smaller mFN fragments are observed upon mGZMB treatment that are absent in the control sample (Figure 6C). The fragments that were generated by mGZMB proteolysis are similar to the fragments generated by hGZMB. However, hGZMB cleaves mFN more effectively as the resulted fragments are of higher intensity. Nevertheless, mGZMB cleaves mFN, leading to dissociation of fragments to the supernatant.

Vascular permeability is reduced in GZMB-KO mice after DTH-induced inflammation

To further confirm the role of GZMB in promoting vascular permeability during inflammation we have induced a DTH reaction on both WT and GZMB-KO mice. In this experiment animals were first sensitized to oxazolone by topical administration on the shaved abdomen. 7 days later ears were challenged and vascular permeability was examined after 24 h and 72 h. Vascular permeability in GZMB-KO mice was significantly lower than WT control, both at the 24 h and 72 h time points (Figure 7). Thus, GZMB deficiency reduced vascular permeability during DTH inflammatory reaction.

Discussion

The ECM exerts a major role in regulating growth factor bioavailability by sequestering and limiting its release [28]. VEGF is a potent vascular permeability agent that is retained in the ECM by binding to FN [10–12]. In the present study, GZMB increased VEGF bioavailability through FN proteolysis. GZMB-mediated VEGF release lead to activation of VEGFR2 in HUVEC. GZMB-mediated vascular leakage *in vivo* is, in part, VEGF-dependent as co-treatment of GZMB and an anti-VEGF neutralizing Ab reduced vascular leakage. Importantly, we have demonstrated the role of GZMB-induced vascular permeability during the development of inflammation as GZMB deficiency reduced vascular leakage in DTH-induced inflammation in mice ears. Thus, GZMB regulates VEGF bioavailability by cleaving FN and promoting vascular leakage during inflammation *in vivo*.

A number of proteases were previously shown to alter VEGF-matrix interaction with significant consequences to vascular morphogenesis. Houck *et al.* were the first to demonstrate that VEGF expressing cells treated with plasmin gave rise to a VEGF fragment that dissociates to the supernatant and is capable of inducing vascular leakage in guinea pig skin [7]. MMP-3 generates an unbound VEGF fragment that promotes the formation of aberrant, dilated and leaky neovessels [8]. On the other hand, MMP-resistant, matrix bound VEGF promoted smaller vessel diameter and highly branched neovessels [8]. These studies highlight the fact that VEGF activity is regulated by its interaction with the ECM, while proteolytic processing of VEGF and its dissociation from the matrix promotes vascular permeability and disrupts normal neovessel formation [35]. As opposed to the

aforementioned proteases, that directly cleave VEGF, generating a smaller VEGF fragment with altered biological activity, VEGF is not a substrate of GZMB. Since GZMB releases VEGF from the ECM, but does not cleave VEGF directly, we predict that GZMB alters VEGF bioavailability through the cleavage of FN in the ECM, leading to the release of the full length VEGF molecule. Indeed, VEGF released from FN by GZMB retain its activity as it leads to VEGFR2 phosphorylation in HUVEC. It will be of interest to explore whether part of the FN molecule remains bound to VEGF after GZMB proteolysis, or whether GZMB completely dissociate VEGF from FN.

Changes in microenvironmental levels of VEGF due to ECM processing may serve as a key mechanism for promoting vascular leakage and pathological angiogenesis in chronic inflammatory diseases [36]. In an elegant study by Ozawa *et al.* it was demonstrated that local low levels of VEGF expression is critical for the formation of stable, non-leaky neovessels, where local high levels of VEGF expression resulted in enlarged, unstable, leaky capillaries that are characteristic of pathological angiogenesis [37]. MMP-9 and MMP-2 induce tumor angiogenesis [38] as well as promote inflammatory angiogenesis by releasing VEGF from the ECM [9]. Moreover, these proteases were shown to promote ovarian ascites formation due to increased VEGF-dependent vascular leakage [39]. However, the role of MMPs in angiogenesis has been challenged by observations suggesting that MMPs are involved in neovessel regression due to the formation of anti-angiogenic protein fragments via ECM proteolysis and by destabilizing EC-matrix interaction through ECM processing [40–43]. Thus, it has been suggested that MMPs serve as local modulators rather than directly induce or suppress angiogenesis [8]. Similarly, we have previously shown that GZMB processing of the ECM disrupt EC-matrix interaction which may pertain to its anti-angiogenic role [26]. Conversely, the current study may suggest that increased VEGF release by GZMB may potentially serve to induce angiogenesis. Although the direct effect of GZMB-mediated VEGF release on angiogenesis has not been examined in this study we suspect that similar to MMPs GZMB may serve as a modulator of the angiogenic response. However, in contrast to MMPs, which play a major role in normal tissue remodeling and homeostasis, elevated GZMB levels are only evident in chronic inflammatory disorders, most of which are highly associated with pathological angiogenesis, including RA, atherosclerosis, AAA and skin pathologies [14, 15]. Given that GZMB increases VEGF bioavailability and induces VEGF-dependent vascular permeability, a hallmark of pathological angiogenesis, we postulate that GZMB contributes to the formation of aberrant, unstable and leaky neovessels through ECM proteolysis and by altering microenvironmental levels of VEGF.

Previous reports indicated that human GZMB and mGZMB are different in their intracellular substrate specificity. As part of their apoptotic inducing activities, human and mouse GZMB were shown to cleave procaspase-3 more efficiently in a species-specific manner [44]. Moreover, the pro-apoptotic protein, Bid, from both human and mouse, is only cleaved by human GZMB but not by mGZMB [44]. In light of these differences in substrate specificity of GZMB between species we ensured to use mGZMB in our *in vivo* experiments. Importantly, we demonstrated that both mouse and human GZMB cleave mouse FN, further corroborating our previous observation on the role of GZMB processing of FN in delaying wound healing in mice [22].

Cumulative evidence supports the role of extracellular GZMB in altering tissue integrity and promoting inflammation through a number of mechanisms. Extracellular GZMB potentiates IL-1α activity by cleaving it and generating an IL-1α fragment that enhances inflammation [24]. We have previously demonstrated that cleavage of fibrillin-1 and decorin by GZMB contributes to AAA rupture in mice [19, 20], while decorin degradation in the skin contributes to skin thinning and frailty [21]. Recently we have demonstrated that GZMB has an indirect effect on tissue remodeling as GZMB promotes the release of active TGF-β from the ECM by cleaving a number of proteoglycans [25]. The current study further corroborates the role of extracellular GZMB in altering growth factor and cytokine release and bioavailability during inflammation. Using the DTH mouse model we observed a significant reduction in vascular permeability in GZMB-KO mice compared to WT control. The DTH inflammatory reaction is mediated by a number of immune cells including T cells, macrophages and mast cell [45]. Release of cytokines and pro-inflammatory agents promote the development of local inflammation in response to a hapten irritant that is applied 7 days post initial sensitization. Importantly, many inflammatory cells that take part in this reaction can express and release GZMB including CD8+ve T cells, mast cells and macrophages [15, 16]. Considering the reduction in vascular permeability due to co-injection of GZMB and anti-VEGF Ab, and the observed reduction in vascular leakage in GZMB deficient mice during local induced inflammation, it can be postulated that extracellular release of GZMB by inflammatory cells promotes vascular permeability mediated by VEGF release from the matrix. Thus, accumulation of extracellular GZMB during chronic inflammation, as observed in a number of chronic diseases [14], may further exacerbate inflammation and delay resolution by promoting vascular permeability.

Previous studies from our laboratory and others suggest that mast cells are a major source of GZMB in the early stages of inflammation [21, 46]. Extracellular release of GZMB from mast cells contributes to cell detachment and disorganization of EC intercellular adherens junctions as a mechanism that may induce vascular leakage [46]; however, evidence for GZMB-mediated vascular leakage was not provided in the latter study. Although we cannot rule out the possibility that GZMB may contribute to vascular leakage by its direct effect on EC in our *in vivo* experiments, the reduction in vascular leakage in mice that were treated with GZMB + anti VEGF neutralizing Ab suggests that GZMB mediates vascular permeability predominantly through altering VEGF bioavailability.

In summary, extracellular GZMB induces VEGF release from the ECM by cleaving FN and promoting vascular permeability during inflammation *in vivo*. This process may serve as a novel mechanism that promotes chronic inflammation in diseases where GZMB is evident while strategies aiming to inhibit GZMB activity may attenuate vascular leakage and reduce the inflammatory response.

Acknowledgments

Sources of support: AH was funded by the Vanier Canada Graduate Scholarship. IH is funded by the Canadian Institutes of Health Research (CIHR) Skin Research Training Scholarship. This work is funded through a grant-in-aid from CIHR.

We would like to thanks Dr. Ed Pryzdial, The Centre for Blood Research, University of British Columbia, for providing plasmin for our experiments.

Abbreviations

ECM	Extracellular matrix
FN	Fibronectin
GZMB	Granzyme B
mGzmb	mouse granzyme B
VEGF	Vascular endothelial growth factor

References

1. Arroyo AG, Iruela-Arispe ML. Extracellular matrix, inflammation, and the angiogenic response. Cardiovasc Res. 2010; 86(2):226–35. [PubMed: 20154066]
2. Nagy JA, Dvorak AM, Dvorak HF. Vascular hyperpermeability, angiogenesis, and stroma generation. Cold Spring Harb Perspect Med. 2012; 2(2):a006544. [PubMed: 22355795]
3. Costa C, Incio J, Soares R. Angiogenesis and chronic inflammation: cause or consequence? Angiogenesis. 2007; 10(3):149–66. [PubMed: 17457680]
4. Nagy JA, Dvorak AM, Dvorak HF. VEGF-A and the induction of pathological angiogenesis. Annu Rev Pathol. 2007; 2:251–75. [PubMed: 18039100]
5. Koch S, Claesson-Welsh L. Signal transduction by vascular endothelial growth factor receptors. Cold Spring Harb Perspect Med. 2012; 2(7):a006502. [PubMed: 22762016]
6. Lee S, Chen TT, Barber CL, et al. Autocrine VEGF signaling is required for vascular homeostasis. Cell. 2007; 130(4):691–703. [PubMed: 17719546]
7. Houck KA, Leung DW, Rowland AM, et al. Dual regulation of vascular endothelial growth factor bioavailability by genetic and proteolytic mechanisms. J Biol Chem. 1992; 267(36):26031–7. [PubMed: 1464614]
8. Lee S, Jilani SM, Nikolova GV, et al. Processing of VEGF-A by matrix metalloproteinases regulates bioavailability and vascular patterning in tumors. J Cell Biol. 2005; 169(4):681–91. [PubMed: 15911882]
9. Ebrahem Q, Chaurasia SS, Vasanji A, et al. Cross-talk between vascular endothelial growth factor and matrix metalloproteinases in the induction of neovascularization in vivo. Am J Pathol. 2010; 176(1):496–503. [PubMed: 19948826]
10. Wijelath ES, Murray J, Rahman S, et al. Novel vascular endothelial growth factor binding domains of fibronectin enhance vascular endothelial growth factor biological activity. Circ Res. 2002; 91(1):25–31. [PubMed: 12114318]
11. Wijelath ES, Rahman S, Namekata M, et al. Heparin-II domain of fibronectin is a vascular endothelial growth factor-binding domain: enhancement of VEGF biological activity by a singular growth factor/matrix protein synergism. Circ Res. 2006; 99(8):853–60. [PubMed: 17008606]
12. Martino MM, Hubbell JA. The 12th–14th type III repeats of fibronectin function as a highly promiscuous growth factor-binding domain. Faseb J. 2010; 24(12):4711–21. [PubMed: 20671107]
13. Martino MM, Tortelli F, Mochizuki M, et al. Engineering the growth factor microenvironment with fibronectin domains to promote wound and bone tissue healing. Sci Transl Med. 2011; 3(100): 100ra89.
14. Hendel A, Hiebert PR, Boivin WA, et al. Granzymes in age-related cardiovascular and pulmonary diseases. Cell Death Differ. 2010; 17(4):596–606. [PubMed: 20139894]
15. Boivin WA, Cooper DM, Hiebert PR, et al. Intracellular versus extracellular granzyme B in immunity and disease: challenging the dogma. Lab Invest. 2009; 89(11):1195–220. [PubMed: 19770840]
16. Hiebert PR, Granville DJ. Granzyme B in injury, inflammation, and repair. Trends Mol Med. 2012; 18(12):732–41. [PubMed: 23099058]

17. Kondo H, Hojo Y, Tsuru R, et al. Elevation of plasma granzyme B levels after acute myocardial infarction. Circ J. 2009; 73(3):503–7. [PubMed: 19145036]
18. Kummer JA, Tak PP, Brinkman BM, et al. Expression of granzymes A and B in synovial tissue from patients with rheumatoid arthritis and osteoarthritis. Clin Immunol Immunopathol. 1994; 73(1):88–95. [PubMed: 7923921]
19. Ang LS, Boivin WA, Williams SJ, et al. Serpina3n attenuates granzyme B-mediated decorin cleavage and rupture in a murine model of aortic aneurysm. Cell Death Dis. 2011; 2:e209. [PubMed: 21900960]
20. Chamberlain CM, Ang LS, Boivin WA, et al. Perforin-independent extracellular granzyme B activity contributes to abdominal aortic aneurysm. Am J Pathol. 2010; 176(2):1038–49. [PubMed: 20035050]
21. Hiebert PR, Boivin WA, Abraham T, et al. Granzyme B contributes to extracellular matrix remodeling and skin aging in apolipoprotein E knockout mice. Exp Gerontol. 2011; 46(6):489–99. [PubMed: 21316440]
22. Hiebert PR, Wu D, Granville DJ. Granzyme B degrades extracellular matrix and contributes to delayed wound closure in apolipoprotein E knockout mice. Cell Death Differ. 2013; 20(10):1404–14. [PubMed: 23912712]
23. Omoto Y, Yamanaka K, Tokime K, et al. Granzyme B is a novel interleukin-18 converting enzyme. J Dermatol Sci. 2010; 59(2):129–35. [PubMed: 20621450]
24. Afonina IS, Tynan GA, Logue SE, et al. Granzyme B-dependent proteolysis acts as a switch to enhance the proinflammatory activity of IL-1alpha. Mol Cell. 2011; 44(2):265–78. [PubMed: 22017873]
25. Boivin WA, Shackleford M, Vanden Hoek A, et al. Granzyme B cleaves decorin, biglycan and soluble betaglycan, releasing active transforming growth factor-beta1. PLoS One. 2012; 7(3):e33163. [PubMed: 22479366]
26. Hendel A, Granville DJ. Granzyme B cleavage of fibronectin disrupts endothelial cell adhesion, migration and capillary tube formation. Matrix Biol. 2013; 32(1):14–22. [PubMed: 23228447]
27. Willoughby CA, Bull HG, Garcia-Calvo M, et al. Discovery of potent, selective human granzyme B inhibitors that inhibit CTL mediated apoptosis. Bioorg Med Chem Lett. 2002; 12(16):2197–200. [PubMed: 12127536]
28. Macri L, Silverstein D, Clark RA. Growth factor binding to the pericellular matrix and its importance in tissue engineering. Adv Drug Deliv Rev. 2007; 59(13):1366–81. [PubMed: 17916397]
29. Keyt BA, Berleau LT, Nguyen HV, et al. The carboxyl-terminal domain (111–165) of vascular endothelial growth factor is critical for its mitogenic potency. J Biol Chem. 1996; 271(13):7788–95. [PubMed: 8631822]
30. Kurtagic E, Jedrychowski MP, Nugent MA. Neutrophil elastase cleaves VEGF to generate a VEGF fragment with altered activity. Am J Physiol Lung Cell Mol Physiol. 2009; 296(3):L534–46. [PubMed: 19136576]
31. Miles AA, Miles EM. Vascular reactions to histamine, histamine-liberator and leukotaxine in the skin of guinea-pigs. J Physiol. 1952; 118(2):228–57. [PubMed: 13000707]
32. Maharaj AS, Saint-Geniez M, Maldonado AE, et al. Vascular endothelial growth factor localization in the adult. Am J Pathol. 2006; 168(2):639–48. [PubMed: 16436677]
33. Elias PM, Arbiser J, Brown BE, et al. Epidermal vascular endothelial growth factor production is required for permeability barrier homeostasis, dermal angiogenesis, and the development of epidermal hyperplasia: implications for the pathogenesis of psoriasis. Am J Pathol. 2008; 173(3): 689–99. [PubMed: 18688025]
34. Xia YP, Li B, Hylton D, et al. Transgenic delivery of VEGF to mouse skin leads to an inflammatory condition resembling human psoriasis. Blood. 2003; 102(1):161–8. [PubMed: 12649136]
35. Ferrara N. Binding to the extracellular matrix and proteolytic processing: two key mechanisms regulating vascular endothelial growth factor action. Mol Biol Cell. 2010; 21(5):687–90. [PubMed: 20185770]

36. Weis SM, Cheresh DA. Pathophysiological consequences of VEGF-induced vascular permeability. Nature. 2005; 437(7058):497–504. [PubMed: 16177780]

37. Ozawa CR, Banfi A, Glazer NL, et al. Microenvironmental VEGF concentration, not total dose, determines a threshold between normal and aberrant angiogenesis. J Clin Invest. 2004; 113(4): 516–27. [PubMed: 14966561]

38. Bergers G, Brekken R, McMahon G, et al. Matrix metalloproteinase-9 triggers the angiogenic switch during carcinogenesis. Nat Cell Biol. 2000; 2(10):737–44. [PubMed: 11025665]

39. Belotti D, Paganoni P, Manenti L, et al. Matrix metalloproteinases (MMP9 and MMP2) induce the release of vascular endothelial growth factor (VEGF) by ovarian carcinoma cells: implications for ascites formation. Cancer Res. 2003; 63(17):5224–9. [PubMed: 14500349]

40. Aplin AC, Zhu WH, Fogel E, et al. Vascular regression and survival are differentially regulated by MT1-MMP and TIMPs in the aortic ring model of angiogenesis. Am J Physiol Cell Physiol. 2009; 297(2):C471–80. [PubMed: 19494241]

41. O'Reilly MS, Wiederschain D, Stetler-Stevenson WG, et al. Regulation of angiostatin production by matrix metalloproteinase-2 in a model of concomitant resistance. J Biol Chem. 1999; 274(41): 29568–71. [PubMed: 10506224]

42. Pozzi A, Moberg PE, Miles LA, et al. Elevated matrix metalloprotease and angiostatin levels in integrin alpha 1 knockout mice cause reduced tumor vascularization. Proc Natl Acad Sci U S A. 2000; 97(5):2202–7. [PubMed: 10681423]

43. Hamano Y, Zeisberg M, Sugimoto H, et al. Physiological levels of tumstatin, a fragment of collagen IV alpha3 chain, are generated by MMP-9 proteolysis and suppress angiogenesis via alphaV beta3 integrin. Cancer Cell. 2003; 3(6):589–601. [PubMed: 12842087]

44. Casciola-Rosen L, Garcia-Calvo M, Bull HG, et al. Mouse and human granzyme B have distinct tetrapeptide specificities and abilities to recruit the bid pathway. J Biol Chem. 2007; 282(7):4545–52. [PubMed: 17179148]

45. Honda T, Egawa G, Grabbe S, et al. Update of immune events in the murine contact hypersensitivity model: toward the understanding of allergic contact dermatitis. J Invest Dermatol. 2013; 133(2):303–15. [PubMed: 22931926]

46. Pardo J, Wallich R, Ebnet K, et al. Granzyme B is expressed in mouse mast cells in vivo and in vitro and causes delayed cell death independent of perforin. Cell Death Differ. 2007; 14(10):1768–79. [PubMed: 17599099]

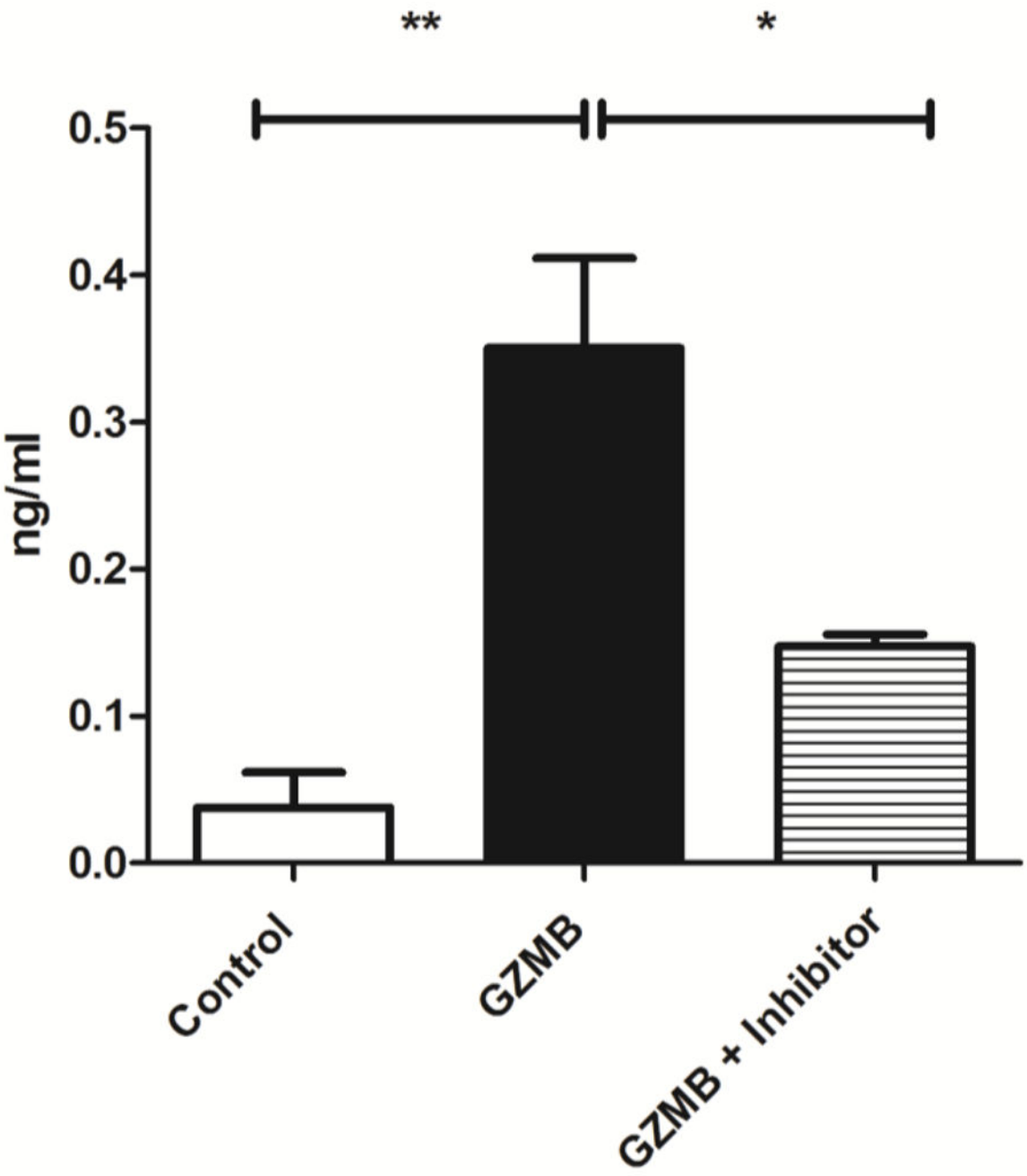

Figure 1.

GZMB releases VEGF from human plasma FN. VEGF (50 ng/ml) was added to FN coated wells and incubated for 2 h at 37 °C. Unbound VEGF was removed by washing with DPBS. GZMB (50 nM) with vehicle control (DMSO) or GZMB with inhibitor (Compound 20; 50 μM) were added to the wells and incubated for 2 h at 37°C. Supernatants were removed and analyzed for VEGF by ELISA. Results are presented as mean ± SEM of n=3 with 3 triplicates per condition (*=P<0.05; ** =P<0.01).

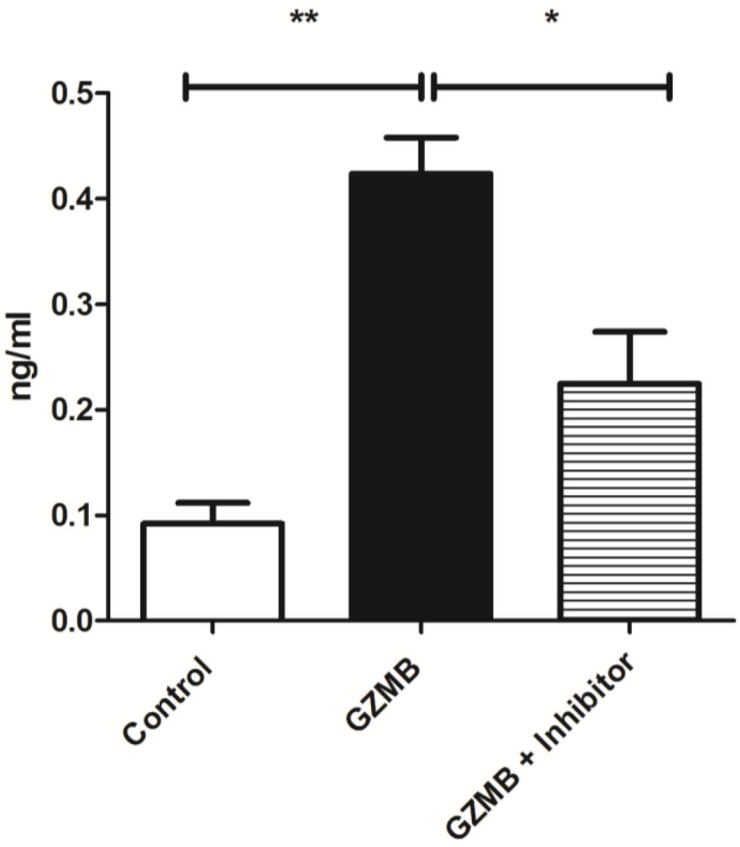

Figure 2.

GZMB releases VEGF from HUVEC matrix. HUVEC were grown to confluence and maintained in serum-reduced media for 9 d. Cells were removed by adding NH_4OH followed by extensive washing. Remaining ECM was incubated with VEGF (50 ng/ml) for 2 h at 37°C. Unbound VEGF was removed by washing with DPBS. GZMB (50 nM) or GZMB with inhibitor (Compound 20, 50 μM) were added and incubated for additional 2 h at 37°C. Supernatants were removed and analyzed for VEGF by ELISA. Results are presented as mean ± SEM of n=3 with 3 triplicates per condition (*P<0.05; ** P<0.01).

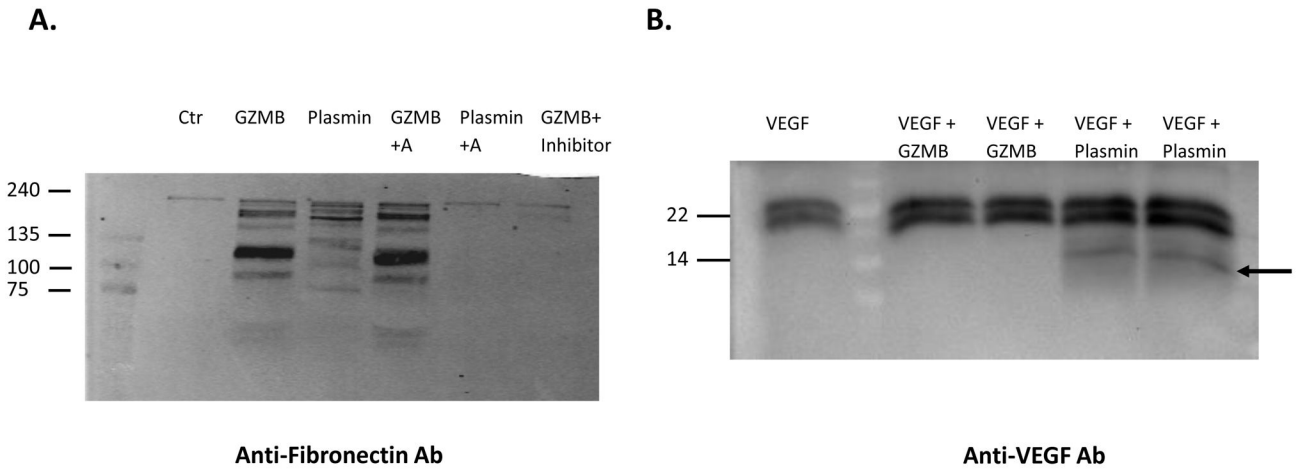

Figure 3.

GZMB degrades FN but does not cleave VEGF. **A**. FN coated culture wells were treated with either GZMB or plasmin (50nM) with or without inhibitors (A, aprotinin) for 2 h at 37 °C. Supernatants were analyzed by western blotting using anti-FN Ab. **B.** Same enzyme preparations used in (A) were incubated with 100ng VEGF in microtubes for 2 h at 37 °C. Samples were analyzed by western blotting using anti-VEGF Ab (arrow denotes VEGF fragment).

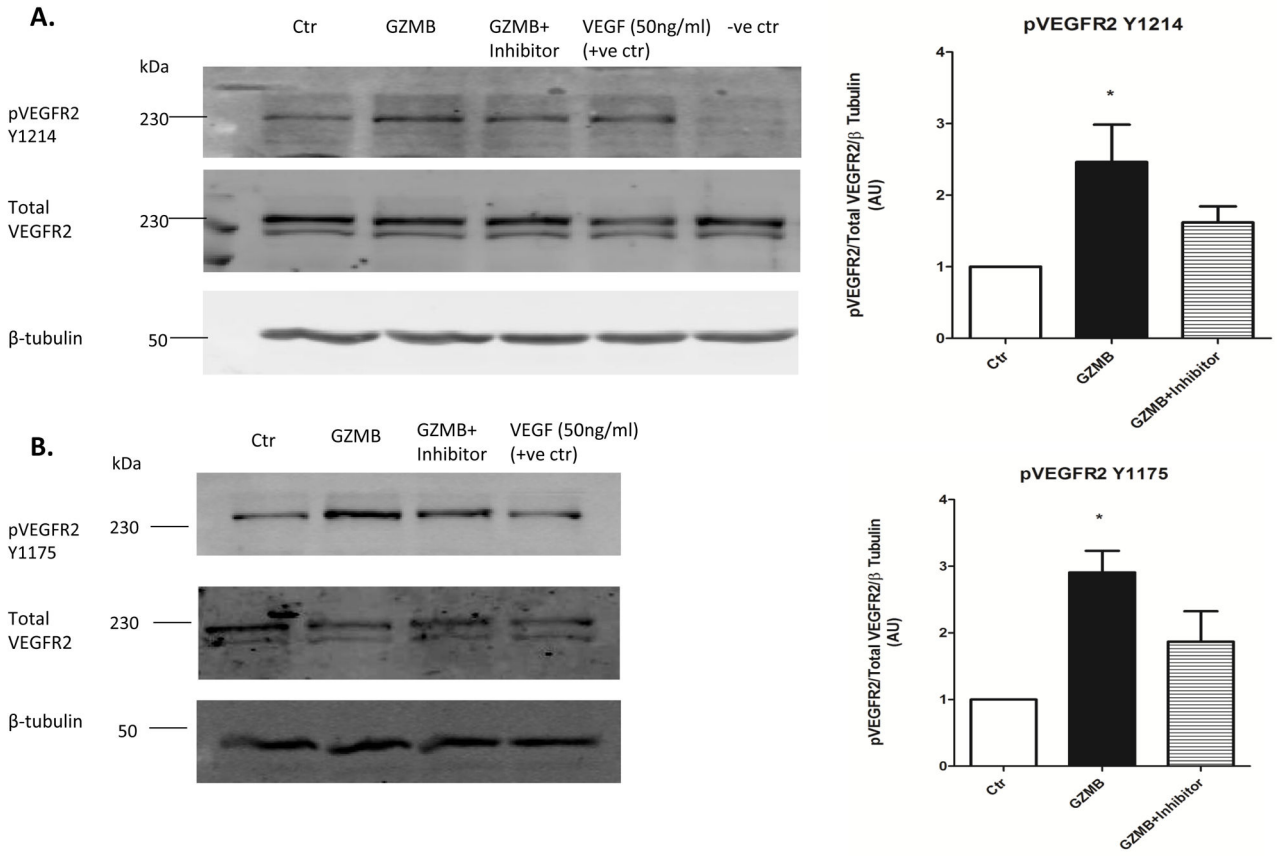

Figure 4.

GZMB-mediated VEGF release from FN activates VEGFR2 in HUVEC. FN coated wells were incubated with VEGF and treated with GZMB or GZMB with inhibitor as in figure 1. Supernatants were removed and added to HUVEC monolayer culture for 7 min. Cell lysates were analyzed by western blotting using **A.** phospho y1214 VEGFR2 Ab (pVEGFR2 y1214) and **B.** phospho y1175 VEGFR2 Ab (pVEGFR2 y1175). HUVEC treated directly with VEGF (50ng/ml) were used as a positive control (+ve ctr). Total VEGFR2 and β-tubulin Abs were used as loading controls. Quantification is presented as the densitometry ratio of pVEGFR2 to total VEGFR2 normalized to β-tubulin. Results are presented as mean ± SEM of n=3 with 3 triplicates per condition (*=P<0.05).

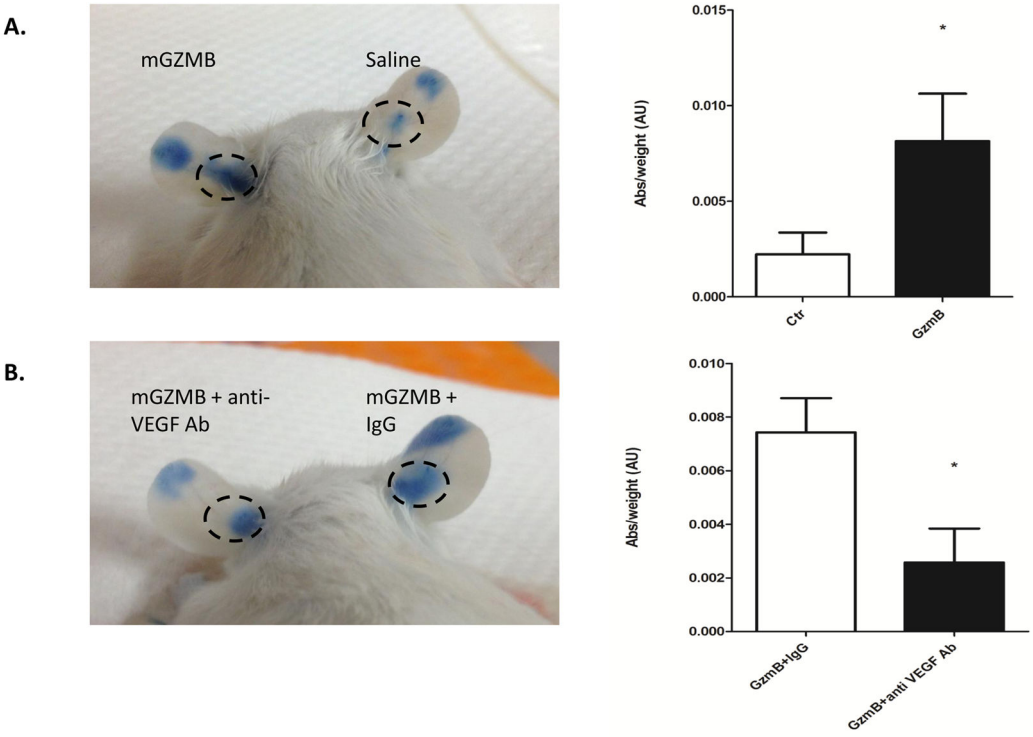

Figure 5.

Mouse Gzmb induces a VEGF-dependent increase in vascular permeability *in vivo*. Evan's blue (0.5%) was injected via the tail vein prior to ear injections of **A.** mGzmb (100 ng) or saline control or **B.** mGzmb with anti-mouse VEGF Ab (1.5 μg) or mGzmb and IgG control Ab (1.5 μg). Ear tissues were excised as indicated using a 7 mm punch biopsy (areas in circle). Evan's blue extraction was performed by drying the tissue and immersing it in formamide at 55°C for 24 h. Results are presented as absorbance (610nm) normalized to tissue weight (mg). Results are presented as mean ± SEM of n=5 (*=P<0.05).

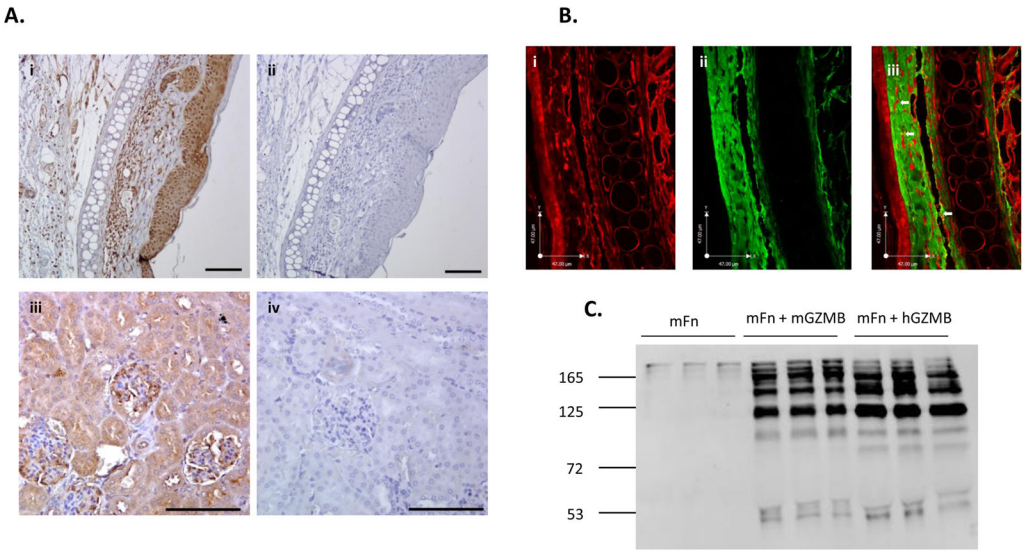

Figure 6.

Endogenous VEGF expression in mouse ear and mGzmb cleavage of murine FN (mFN). **A.** Untreated mouse ears were analyzed for endogenous mouse VEGF expression using immunohistochemistry with anti-mouse VEGF Ab (i). Mouse kidney sections were used as positive control for VEGF staining (iii). Ear section (ii) or kidney section (iv) stained without primary antibody were used as negative controls. Scale bar= 100μm. **B.** Double immunofluorescence using anti-mouse VEGF Ab (i, red) and anti-FN Ab (ii, green) demonstrating co-localization of VEGF and FN (iii, overlay, arrows) in the deep dermis. Scale bar = 47 μm. **C.** Culture wells coated with mFN were treated with either mGzmb or human GZMB (hGZMB) and incubated for 2 h at 37°C. Supernatants were removed and analyzed by western blotting using anti-FN Ab.

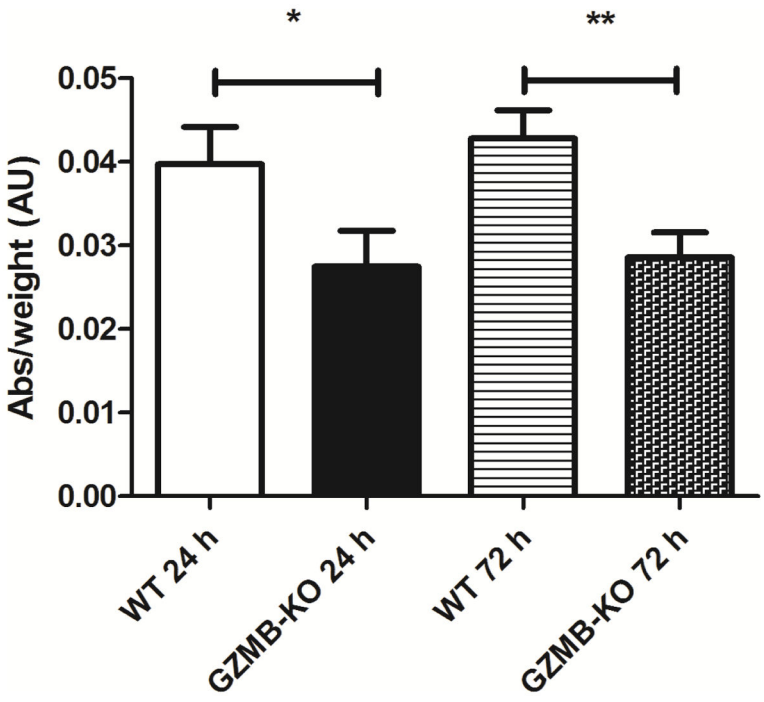

Figure 7.

Vascular permeability is reduced in GZMB-KO mice after DTH-induced inflammation. WT and GZMB-KO mice were challenged with topical administration of oxazolone to both ears 7 days post initial sensitization leading to the development of DTH inflammatory reaction in the ear. At the indicated time points Evans blue was injected and ears were harvested followed by dye extraction to asses vascular permeability as indicated in Materials and Methods. Results are presented as mean ± SEM. 24h WT n=8; GZMB-KO n=11; 72h WT n= 11; GZMB-KO n=7. (*=P<0.05; **=P<0.01).